

1-1-2009

Non-collinear generation of third harmonic of IR ultrashort laser pulses by PTR glass volume Bragg gratings

Leo A. Siiman
University of Central Florida

Julien Lumeau
University of Central Florida

Lionel Canioni

Leonid B. Glebov
University of Central Florida

Find similar works at: <https://stars.library.ucf.edu/facultybib2000>
University of Central Florida Libraries <http://library.ucf.edu>

This Article is brought to you for free and open access by the Faculty Bibliography at STARS. It has been accepted for inclusion in Faculty Bibliography 2000s by an authorized administrator of STARS. For more information, please contact STARS@ucf.edu.

Recommended Citation

Siiman, Leo A.; Lumeau, Julien; Canioni, Lionel; and Glebov, Leonid B., "Non-collinear generation of third harmonic of IR ultrashort laser pulses by PTR glass volume Bragg gratings" (2009). *Faculty Bibliography 2000s*. 2144.

<https://stars.library.ucf.edu/facultybib2000/2144>

Non-collinear generation of third harmonic of IR ultrashort laser pulses by PTR glass volume Bragg gratings

Leo A. Siiman^a, Julien Lumeau^a, Lionel Canioni^b, Leonid B. Glebov^a

^aCREOL/The College of Optics and Photonics, University of Central Florida
P.O. Box 162700 Orlando, FL 32816-2700, USA

^bCPMOH, University of Bordeaux I, 351 Cours de la Liberation, 33405 Talence cedex, France
lsiiman@creol.ucf.edu

Abstract: Three conditions for non-collinear third harmonic generation by a PTR glass volume Bragg grating are demonstrated using infrared ultrashort pulse illumination. Each condition corresponds to a different angle of grating orientation and a separate generation mechanism. We identify the mechanisms as corresponding to sum-frequency generation, Bragg diffraction of 3ω , and a non-resonant Bragg condition involving three ω photons interacting with a nonlinear grating vector. Theoretical modeling is performed using wave vector additions and the results are compared to experimental measurements.

©2009 Optical Society of America

OCIS codes: (190.4720) Optical nonlinearities of condensed matter; (320.2250) Femtosecond phenomena; (160.5335) Photosensitive materials; (050.7330) Volume gratings

References and links

1. O. M. Efimov, L.B. Glebov, and V. I. Smirnov, "High-frequency Bragg gratings in a photothermorefractive glass," *Opt. Lett.* **25**, 1693-1695 (2000).
2. L. B. Glebov, V. I. Smirnov, C. M. Stickley, and I. V. Ciapurin, "New approach to robust optics for HEL systems," *Proc. SPIE* **4724**, 101-109 (2002).
3. L. B. Glebov, L. N. Glebova, V. I. Smirnov, M. Dubinskii, L. D. Merkle, S. Papernov, and A.W. Schmid, "Laser Damage Resistance of Photo-Thermo-Refractive Glass Bragg Gratings," *Proceedings of Solid State and Diode Lasers Technical Review*. Albuquerque, Poster-4 (2004).
4. V. I. Smirnov, S. Juodkazis, V. Dubikovskiy, J. Hales, B. Ya. Zel'dovich, H. Misawa, and L. B. Glebov, "Resonant third harmonic generation by femtosecond laser pulses on Bragg grating in photosensitive silicate glass," *Conference on Lasers and Electro-Optics CLEO-2002 paper CTuG7* (2002).
5. S. Juodkazis, E. Gaizauskas, V. Jarutis, J. Reif, S. Matsuo and H. Misawa, "Optical third harmonic generation during femtosecond pulse diffraction in a Bragg grating," *J. Phys. D: Appl. Phys.* **39**, 50 (2006).
6. H. Kogelnik, "Coupled wave theory for thick hologram gratings," *Bell. Syst. Tech. J.* **48**, 2909 (1969).
7. I. V. Ciapurin, L. B. Glebov, and V. I. Smirnov, "Modeling of Gaussian beam diffraction on volume Bragg gratings in PTR glass," *Proc. SPIE* **5742**, 183-194 (2005).
8. J. X. Cheng and X. S. Xie, "Green's function formulation for third-harmonic generation microscopy," *J. Opt. Soc. Am. B* **19**, 1604-1610 (2007).

1. Introduction

1.1 PTR Glass

Photo-thermo refractive (PTR) glass is a sodium-zinc-aluminum-silicate glass containing small amounts of fluorine and bromine, doped with cerium, silver, antimony, and tin. Exposure to ultraviolet light followed by heat treatment leads to a precipitation of sodium fluoride dielectric nanocrystals in the glass. These crystals induce a decrease in refractive index by as much as 10^{-3} (1000 ppm) and are associated with low losses. This photosensitivity is sufficient for recording high efficiency Bragg gratings in PTR glass samples having thicknesses of a few millimeters [1]. PTR glass has no intrinsic absorption in the near IR spectral region. Therefore its laser damage threshold is high for both CW and pulsed irradiation. Experiments have shown that PTR glass tolerates up to 100 kW/cm^2 of CW

irradiation by a 1085 nm Yb-doped fiber laser focused to a spot diameter of 300 μm [2]. The laser damage threshold of a volume Bragg grating recorded in PTR glass for a focused single mode 1 nsec pulse at 1064 nm is 20 J/cm², but is locally decreased to 7 J/cm² when Pt inclusions are present [3]. The high laser damage threshold of PTR glass volume Bragg gratings make them ideal for use in high power laser systems.

1.2 THG by a volume Bragg grating in PTR glass

Non-collinear third harmonic generation (THG) by a volume transmitting Bragg grating (TBG) in PTR glass under high-intensity femtosecond pulse irradiation near 800 nm was first observed by Smirnov et al. when a TBG was placed at Bragg angle for the fundamental wavelength [4]. In addition to the expected transmitted and diffracted beams, two THG beams with propagation directions corresponding to the condition of sum-frequency generation (SFG) were observed. However the phase matching condition for SFG was not satisfied. A possible explanation in terms of self-phase matching via Cherenkov radiation has been recently proposed [5]. One limitation of this experimental configuration is that the use of femtosecond pulses near 800 nm places THG in the ultraviolet regime and within the absorption region of PTR glass. This configuration prevents propagation of surface or bulk third harmonic inside the PTR glass and therefore does not allow for a complete study of the THG phenomena. Investigation of THG by a TBG in PTR glass at third harmonics within the transparency range of PTR glass requires fundamental pulses longer than 1000 nm. In this paper we discuss experiments dealing with THG by a TBG in PTR glass using ultrashort laser pulses at 1300 nm and 1588 nm. The original case of two THG beams for the grating at Bragg angle is again observed at these wavelengths. We consider the angular dependence of the intensity of these two beams and derive a model that supports a SFG interaction. In addition to THG at Bragg angle for fundamental, two new angular orientations of the TBG are shown to produce non-collinear third harmonic generation. We provide theoretical explanations to account for these new angles.

2. Experimental observations

It is instructive to review the case of THG for femtosecond pulses near 800 nm interacting with a TBG in PTR glass. A Ti:sapphire regenerative amplifier laser system was used to generate femtosecond pulses with the following parameters: pulsewidth ~ 120 fsec, repetition rate 1 kHz, central wavelength at 780 nm and pulse energies up to 1 mJ. The beam was focused by a lens with focal length equal to 1 m. A TBG with spatial period 4 μm , thickness 0.85 mm, and amplitude of refractive index modulation 467 ppm, was placed near the focal plane. Figure 1 shows the experimental arrangement.

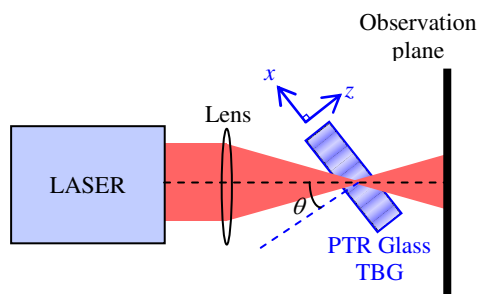


Fig. 1. Experimental arrangement for investigating third harmonic generation and diffraction by transmitting Bragg gratings in PTR glass.

The angle θ of the TBG was set to Bragg angle for 780 nm and calculated according to Bragg's law

$$\sin \theta = \frac{\lambda}{2n(\lambda)\Lambda}, \quad (1)$$

where $n(\lambda)$ is the refractive index of PTR glass as a function of wavelength and Λ is the spatial period of the grating. Figure 2 shows that after propagation through the TBG, two THG beams, $3\omega^{(i)}$ and $3\omega^{(ii)}$, appeared between the diffracted, ω_D , and transmitted, ω_T , beams. We call this configuration two-beam THG and distinguish the beams by labeling THG closest to the transmitted beam as $3\omega^{(i)}$ and THG closest to the diffracted beam as $3\omega^{(ii)}$.

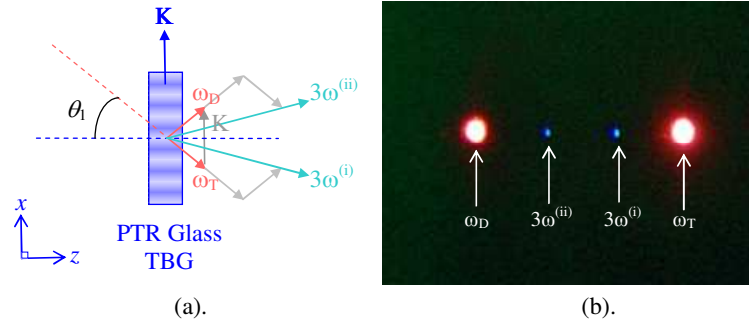


Fig. 2. Two-beam THG by a PTR glass TBG irradiated with IR femtosecond pulses: (a) wave vector additions of transmitted and diffracted photons to produce third harmonic (b) photograph from experiment. \mathbf{K} – grating vector, ω_T – transmitted photon, ω_D – diffracted photon. Phase-matching is not satisfied.

The beams appear blue on the white paper observation plane because ultraviolet photons cause luminescence of chemicals in the paper. Spectral measurement with an Ocean Optics spectrometer confirmed that the THG beams are at 266 nm. Figure 2(a) shows that the direction of the two THG beams is determined by assuming a SFG interaction between transmitted and diffracted photons, i.e. two transmitted photons plus one diffracted photon or vice versa. For this grating spatial period ($4\ \mu\text{m}$) and wavelength of irradiation (780 nm) no other angles were observed to generate non-collinear THG. To further investigate the phenomena of THG by PTR glass gratings we extended our study to include ultrashort laser pulses at longer wavelengths. The wavelength dependence of THG was tested with an optical parametric amplifier (OPA) laser system (pulsewidth < 200 fsec, pulse energies up to 0.1 mJ, and repetition rate at 1 kHz) that generated femtosecond pulses at 1300 nm and 1588 nm. Long focal length lenses focused the femtosecond beam in order to achieve intensity at the focal point on the order of 10^{12} W/cm². A TBG in PTR glass with $4\ \mu\text{m}$ spatial period, 0.97 mm thickness, and amplitude of refractive index modulation of 607 ppm was placed near the focal plane. The angles of the TBG at which non-collinear THG was generated were measured and given in Table 1. At the wavelengths 1300 nm and 1588 nm, it was again observed that for the TBG oriented at Bragg angle for fundamental, two THG beams appeared between the transmitted and diffracted beams. We will designate the Bragg angle for fundamental as θ_1 . However, in addition to THG at θ_1 two other angles also resulted in non-collinear generation of third harmonic. These two interactions are illustrated in Figs. 3(a)&(b) along with the assumed wave vector conditions responsible for their generation. At angle θ_2 , THG is attributed to Bragg diffraction for incident light at wavelength $\lambda/3$. This interaction is likely due to the generation of third harmonic at the front interface of the glass grating and then subsequent diffraction of this surface generated third harmonic. This phenomenon could not be seen with fundamental pulses at 780 nm because of absorption of 266 nm light in the bulk of PTR glass after generation by the front surface.

Table 1. Measured angles for non-collinear THG by a TBG in PTR glass ($\Lambda = 4 \mu\text{m}$, $L = 0.97 \text{ mm}$, $n_1 = 607 \text{ ppm}$).^a

Angle	Wavelength	
	1300 nm	1588 nm
θ_1	9.8°	11.5°
θ_2	3.5°	3.4°
θ_3	14.8°	7.7°
$-\theta_3$	-14.3°	-8.3°
$-\theta_2$	-2.9°	-3.9°
$-\theta_1$	-9.6°	-11.8°

^aAccuracy of angular measurements $\pm 0.5^\circ$.

We designate THG at angle θ_2 as surface diffracted THG. The appearance of THG at angle θ_3 represents a non-Bragg resonance condition where three fundamental photons interact with a grating vector to generate the third harmonic. We label the THG process at angle θ_3 as generation and diffraction by a nonlinear grating. In the next section we impose phase-matching conditions on the three assumed wave vector interactions and derive theoretical values for the angles at which THG is expected. A comparison of these theoretical values is then done with the experimentally measured values of Table 1.

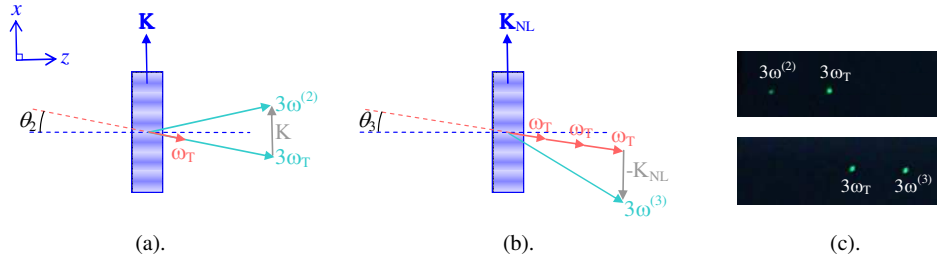


Fig. 3. Wave vector conditions for non-collinear THG by a PTR glass TBG: (a) front surface diffracted THG (b) nonlinear grating THG, \mathbf{K}_{NL} – nonlinear grating vector (c) photographs of $3\omega^{(2)}$ and $3\omega^{(3)}$ from experiment at 1588 nm.

3. Phase-matching conditions

There are three interactions with a TBG in PTR glass that exhibit non-collinear THG under high-intensity femtosecond irradiation. For the two-beam THG interaction shown in Fig. 2(a) the assumed SFG wave vector equations can be written as

$$\mathbf{k}_{3\omega^{(i)}} = 2\mathbf{k}_T(\lambda, \theta) + \mathbf{k}_D(\lambda, \theta), \quad (2)$$

$$\mathbf{k}_{3\omega^{(ii)}} = \mathbf{k}_T(\lambda, \theta) + 2\mathbf{k}_D(\lambda, \theta), \quad (3)$$

where the transmitted wave vector $\mathbf{k}_T(\lambda, \theta)$ and the diffracted wave vector $\mathbf{k}_D(\lambda, \theta)$ are given by

$$\mathbf{k}_T(\lambda, \theta) = \mathbf{k}(\lambda, \theta), \quad (4)$$

$$\mathbf{k}_D(\lambda, \theta) = \mathbf{k}(\lambda, \theta) + \mathbf{K}, \quad (5)$$

and the incident wave vector $\mathbf{k}(\lambda, \theta)$ and grating vector \mathbf{K} are

$$\mathbf{k}(\lambda, \theta) = \frac{2\pi}{\lambda} n(\lambda) [\sin \theta \hat{\mathbf{x}} + \cos \theta \hat{\mathbf{z}}], \quad (6)$$

$$\mathbf{K} = \frac{2\pi}{\Lambda} \hat{\mathbf{x}}. \quad (7)$$

The refractive index of PTR glass as a function of wavelength is given by a Cauchy fit of the form

$$n(\lambda) = \sqrt{A + B\lambda^2 + C\lambda^{-2} + D\lambda^{-4} + E\lambda^{-6} + F\lambda^{-8}}, \quad (8)$$

where λ is expressed in microns and the values of A, B, C, D, E and F are given in Table 2.

Table 2. Cauchy coefficients for PTR glass.

Coefficient	Value	Units
A	2.20959×10^0	
B	-9.71400×10^{-3}	μm^{-2}
C	9.99400×10^{-3}	μm^2
D	1.37070×10^{-4}	μm^4
E	-2.40635×10^{-6}	μm^6
F	-2.96604×10^{-7}	μm^8

In order for the wave vectors given by Eqs. (2) & (3) to be phase-matched their magnitude must equal the magnitude of a third harmonic wave vector, i.e.

$$k_{3\omega} = k(\lambda/3, \theta) = 3 \left(\frac{2\pi}{\lambda} \right) n(\lambda). \quad (9)$$

However, when the laser and grating parameters used to generate the THG beams seen in Fig. 1(b) are substituted into Eq. (9) we have a mismatch. In general there will always be a mismatch. This suggests that the SFG assumption which Eqs. (2) & (3) represent is wrong. Nevertheless the SFG assumption proves useful for studying the intensity dependence of the two THG beams as a function of angle as will be shown in the next section. For now let us continue to analyze the phase-matching conditions and look at the other two cases where THG was observed. To check phase-matching for the wave vector interactions at angle θ_2 and θ_3 we write

$$\mathbf{k}_{3\omega(2)} = \mathbf{k}(\lambda/3, \theta) + \mathbf{K}, \quad (10)$$

$$\mathbf{k}_{3\omega(3)} = 3\mathbf{k}(\lambda, \theta) + \mathbf{K}_{\text{NL}}. \quad (11)$$

Eq. (10) relates to the case seen in Fig. 3(a) and Eq. (11) relates to the case seen in Fig. 3(b). It is necessary to introduce a nonlinear grating vector \mathbf{K}_{NL} because the three photon interaction is a χ_3 process that interacts with the nonlinear refractive index n_2 and not the linear refractive index for which the grating vector \mathbf{K} is defined for. Nevertheless we evaluate both \mathbf{K} and \mathbf{K}_{NL} using Eq. (7). This implicitly assumes grating modulation of the nonlinear index follows the modulation in the linear refractive index. The angle θ in each of the above wave vector equations is solved for by imposing the phase-matching condition given by Eq. (9). The grating we label the angles that satisfy Eqs. (10) & (11) as θ_2 and θ_3 respectively. The resulting solutions are for angles inside a medium of refractive index n and are converted to angles in air by Snell's law

$$\theta = \sin^{-1} \left[n \sin \theta_{\text{media}} \right]. \quad (12)$$

Table 3 shows that the theoretical angles θ_2 and θ_3 agree with the experimentally measured values. Also, the theory is able to account for the large change in angle θ_3 as the wavelength changed from 1300 nm to 1588 nm. Hence we have justified the assumed wave vector equations given by Eqs. (10) & (11). The theoretical angle for θ_1 is derived from Eq. (1), but the argument for a SFG interaction that causes two-beam THG will be made in the next section that discusses the angular selectivity of each of the THG beams.

Table 3. Theoretically derived and experimentally measured angles of grating orientation to obtain non-collinear THG for a PTR glass TBG ($\Lambda = 4 \mu\text{m}$, $L = 0.97 \text{ mm}$, $n_1 = 607 \text{ ppm}$).

Angle	$\lambda = 1300 \text{ nm}$		$\lambda = 1588 \text{ nm}$	
	Experiment	Theory	Experiment	Theory
θ_1	9.8°	9.36°	11.5°	11.45°
θ_2	3.5°	3.1°	3.4°	3.8°
θ_3	14.8°	14.4°	7.7°	8.2°
$-\theta_3$	-14.3°	-14.4°	-8.3°	-8.2°
$-\theta_2$	-2.9°	-3.1°	-3.9°	-3.8°
$-\theta_1$	-9.6°	-9.36°	-11.8°	-11.45°

4. Angular selectivity of two-beam THG

It was seen in the last section that phase-matching assuming SFG is not satisfied for the two-beam THG condition at angle θ_1 . Let us see if we can support an SFG interaction by measuring the angular selectivity of the two THG beams. Angular detuning from Bragg condition affects the relative intensities of transmitted and diffracted beams. Therefore, if THG is a result of interaction between transmitted and diffracted photons, the intensities of the THG beams will be affected differently. A Ti:sapphire regenerative amplifier laser system operating at 780 nm, ~120 fsec, 1 kHz, and pulse energies up to 1 mJ was used with a TBG with the following parameters: $\Lambda = 4 \mu\text{m}$, $L = 0.85 \text{ mm}$, $n_1 = 467 \text{ ppm}$. A computer controlled rotation stage controlled the angle of the TBG while an amplified GaP photodetector measured the intensity of THG. Due to the bandwidth sensitivity of the detector, no light was detected from transmitted or scattered fundamental radiation, and only radiation from THG was detected. Figure 4 shows the experimentally obtained angular selectivity profiles for the two THG beams. It is evident that the $3\omega^{(i)}$ and $3\omega^{(ii)}$ beams show different angular dependencies.

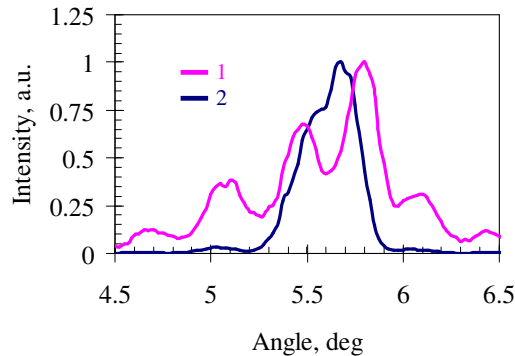


Fig. 4. Dependence of third harmonic intensity from PTR glass TBG on incident angle for (1) $3\omega^{(i)}$ beam (2) $3\omega^{(ii)}$ beam.

To model the angular selectivity of third harmonic generation for the two-beam THG case let us assume SFG interactions. We can then write the intensity of THG for each of the beams as

$$I_{3\omega^{(i)}} = \kappa I_{\omega_T} I_{\omega_T} I_{\omega_D}, \quad (13)$$

$$I_{3\omega^{(ii)}} = \kappa I_{\omega_D} I_{\omega_D} I_{\omega_T}, \quad (14)$$

where κ is a constant, I_{ω_T} is the intensity of the transmitted beam and I_{ω_D} is the intensity of the diffracted beam. Assuming that the spectral selectivity of the TBG is larger than the bandwidth of the laser it is possible to neglect the integration between the spectral profile of the beam and the diffraction efficiency of the TBG. When the grating selectivity is greater than the laser spectral bandwidth the intensity of the diffracted and transmitted beams can be written as

$$I_{\omega_D} = I_0 \eta(\theta), \quad (15)$$

$$I_{\omega_T} = 1 - I_{\omega_D}, \quad (16)$$

where I_0 is the incident intensity and $\eta(\theta)$ is the diffraction efficiency of the TBG as a function of incident angle. The behavior of volume Bragg gratings is well modeled using Kogelnik's coupled wave theory [6]. The diffraction efficiency for a TBG at resonant frequency is

$$\eta(\theta) = \frac{\sin^2 \left\{ \sqrt{\nu^2(\theta) + \xi^2(\theta)} \right\}}{1 + \xi^2(\theta)/\nu^2(\theta)}, \quad (17)$$

where

$$\nu(\theta) = \frac{\pi n_1 L}{\lambda \cos \theta}, \quad (18)$$

$$\xi(\theta) = \frac{z}{2 \cos \theta} \left[K \sin \theta - \frac{K^2 \lambda}{4\pi n(\lambda)} \right]. \quad (19)$$

We multiplied Eq. (17) by a constant factor of 0.7 because the maximum experimental diffraction efficiency did not reach 100% as predicted theoretically due to a limited interaction distance in the TBG and divergence of the beam resulting in integration of the diffraction efficiency over several incidences [7]. We then solved for the theoretical THG intensities, Eqs. (13) & (14). Figure 5 shows how the theoretical solutions compare to the experimentally measured THG intensities. It is seen that the theoretical model produces angular profiles for $3\omega^{(i)}$ and $3\omega^{(ii)}$ that account for the main intensity fluctuations seen in the experimental measurements. Lobe maxima and minima are in agreement for both experiment and theory. The model however does not predict the asymmetry seen in the experimental measurements. This asymmetry can be a consequence of the asymmetry of the fundamental pulse spectrum, shown in Fig. 6, which was used for performing these THG experiments.

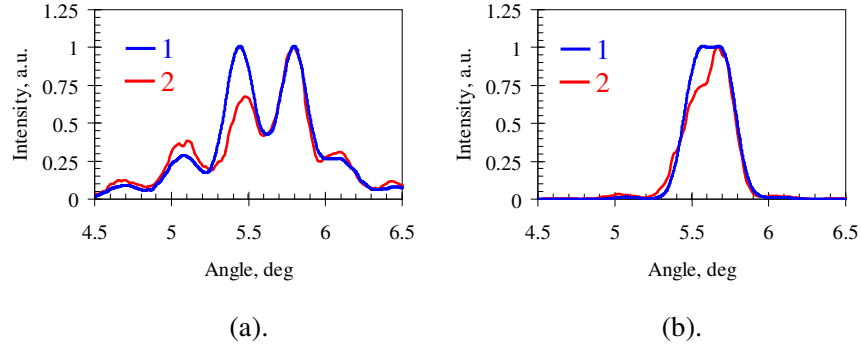


Fig. 5. Dependence of third harmonic intensity on incident angle for the two-beam THG case: (a) $3\omega^{(i)}$ beam (b) $3\omega^{(ii)}$ beam. 1 – theory 2 – experiment.

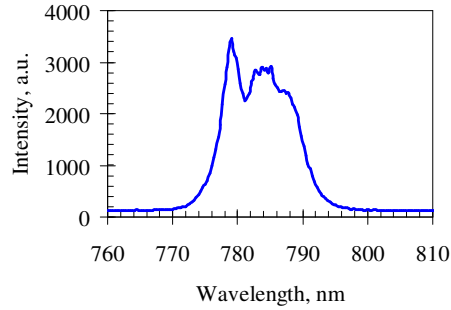


Fig. 6. Spectrum of femtosecond pulse shows an asymmetric profile.

5. Nonlinear refractive index grating

The resonant process assumed in Eq. (11) that determines the angle θ_3 and generates THG requires three fundamental photons to interact with a grating vector. This is a χ_3 process and no interaction can occur with the linear grating vector of the TBG recorded inside PTR glass. Therefore the interaction occurs between the incident wave vectors and a grating vector arising from the nonlinear contribution of χ_3 . This is possible if we assume that modulation in χ_3 occurs concurrently with modulation in the linear refractive index. The nonlinear susceptibility can then be written as

$$\chi_3 = \chi_3^{(0)} + \delta\chi_3^{(0)} \exp(i\mathbf{K}_{\text{NL}} \cdot \mathbf{r}), \quad (20)$$

showing a static part and a modulated part that depends on the nonlinear grating vector \mathbf{K}_{NL} . Using a Green's formulation [8] to solve the nonlinear wave equation gives a solution of the form

$$\mathbf{E}_{3\omega} \propto \iiint \exp(i\mathbf{k}_{3\omega} \cdot \mathbf{r}) \mathbf{P}_{3\omega} d^3\mathbf{r}, \quad (21)$$

where

$$\mathbf{P}_{3\omega} = \chi_3 \mathbf{E}_1 \mathbf{E}_2 \mathbf{E}_3. \quad (22)$$

For the case of angle θ_3 with three incident fundamental photons we can write the electric fields as

$$\mathbf{E}_1 = \mathbf{E}_2 = \mathbf{E}_3 = \mathbf{E}_0 \exp(-i \mathbf{k}_\omega \cdot \mathbf{r}), \quad (23)$$

and after substitution into Eq. (22) we arrive at

$$\begin{aligned} \mathbf{E}_3 \propto & \int_V \chi_3^{(0)} E_0^3 \exp[i(\mathbf{k}_{3\omega} - 3\mathbf{k}_\omega) \cdot \mathbf{r}] d^3 \mathbf{r} \\ & + \int_V \delta \chi_3^{(0)} E_0^3 \exp[i(\mathbf{k}_{3\omega} - 3\mathbf{k}_\omega + \mathbf{K}_{\text{NL}}) \cdot \mathbf{r}] d^3 \mathbf{r}. \end{aligned} \quad (24)$$

In order for phase-matching to occur the argument of the exponentials must go to zero. In the first integral this is not possible because of PTR glass dispersion. However, in the second integral the nonlinear grating vector can compensate for dispersion mismatch and we have the condition

$$(\mathbf{k}_{3\omega} - 3\mathbf{k}_\omega + \mathbf{K}_{\text{NL}}) \cdot \mathbf{r} = 0. \quad (25)$$

Since we expect that the change in nonlinear refractive index follows the change in linear refractive index we can equate \mathbf{K}_{NL} with \mathbf{K} . In this case Eq. (25) is equivalent to Eq. (11). Thus the THG condition given by Eq. (11) is justified by assuming a nonlinear grating arising from modulation in χ_3 in PTR glass. The Green's formulation was applied to explain the nonlinear THG but is not limited to this case. It is also possible to formulate the SFG interaction and derive Eqs. (2) & (3). We write the electric fields in the case of SFG involving two transmitted photons and one diffracted photon as

$$\mathbf{E}_1 = \mathbf{E}_2 = \mathbf{E}_0 \exp(-i \mathbf{k}_T \cdot \mathbf{r}), \quad (26)$$

$$\mathbf{E}_3 = \mathbf{E}_0 \exp(-i \mathbf{k}_D \cdot \mathbf{r}). \quad (27)$$

Then after substitution into Eqs. (22) & (21) we have

$$\begin{aligned} \mathbf{E}_3 \propto & \int_V \chi_3^{(0)} E_0^3 \exp[i(\mathbf{k}_{3\omega} - 2\mathbf{k}_T - \mathbf{k}_D) \cdot \mathbf{r}] d^3 \mathbf{r} \\ & + \int_V \delta \chi_3^{(0)} E_0^3 \exp[i(\mathbf{k}_{3\omega} - 2\mathbf{k}_T - \mathbf{k}_D + \mathbf{K}_{\text{NL}}) \cdot \mathbf{r}] d^3 \mathbf{r}. \end{aligned} \quad (28)$$

Equating the argument in the first integral to zero we obtain

$$(\mathbf{k}_{3\omega} - 2\mathbf{k}_T - \mathbf{k}_D) \cdot \mathbf{r} = 0. \quad (29)$$

which is identical to Eq. (2). Likewise Eq. (3) can be derived in a similar manner by assuming the electric fields involve two diffracted photons and one transmitted photon. However, as was seen previously, Eq. (2) is not phase-matched and therefore Eq. (29) is not exactly equal to zero. This *unphase*-matched THG leads to low conversion efficiency. The efficiency of THG for the SFG interaction was estimated using the responsivity of GaP photodetectors to be on the order of 10^{-4} . A larger conversion efficiency would be expected for volume gratings

in phosphate glasses rather than alkali-silicate glasses such as PTR glass because of higher third-order susceptibility $\chi_3^{(0)}$ in those glasses.

6. Conclusion

We have shown new conditions for THG from a TBG in PTR glass irradiated by high intensity infrared femtosecond pulses. The two new interactions correspond to Bragg diffraction at 3ω and a three photon interaction with the modulated nonlinear refractive index of PTR glass. We also measured the angular selectivity of THG for the two-beam THG condition and showed that a SFG interaction can explain the experimental angular profiles.

Acknowledgments

The authors would like to acknowledge National Science Foundation's support through the International Materials Institute for New Functionality in Glass (Grant No. DMR-0409588) and Arnaud Royon for fruitful discussions about third harmonic generation in amorphous materials.